Natalia KONCHAKOVA*, Ralf MUELLER*, Franz-Josef BARTH*

MODELLING OF DAMAGE EVOLUTION IN ADHESIVE METAL-COMPOSITE STRUCTURES FOR VARIOUS JOINT DESIGNS

SUMMARY

A viscoelastic model with the Lemaitre-type damage is applied to simulate the mechanical behaviour of the contact zone of an adhesive aluminum/fiber-reinforced polymer specimen. The damage evolution in this light weight engineering structure is investigated. The joints of aluminium alloy 5754 (AA5754) and carbon fibre reinforced thermoplastic composite CF-PA66 are manufactured by means of adhesion with an epoxy (1K-EP). The contact zone is considered as an interface material. The aim of the research is to study the influence of the interface geometry on the mechanical characteristics of the structure. The finite element method is used to simulate the complex processes in the joint. The aluminium substrate is modeled as an elastoplastic continuum with linear (isotropic) hardening. The polymer composite possesses an orthotropic elastic behaviour. A solid interface approach is used for the discretisation of the damage domain. It is shown that damage evolution depends on the geometry of the interface. The present work contains the numerical analysis of fracture processes in adhesive specimens with square, rectangular- and circle-shaped geometry of the joint.

Keywords*: Damage, Finite element analysis, Viscoelasticity, Lemaitre-type damage, Metal/composite joint*

MODELOWANIE EWOLUCJI USZKODZENIA W ADHEZYJNYCH UKŁADACH METAL-KOMPOZYT DLA RÓŻNEJ GEOMETRII POŁĄCZENIA

Lepkosprężysty model z uszkodzeniem typu Lemaitre'a jest stosowany w symulacji zachowania strefy kontaktu adhezyjnego w próbce glinu połączonego z polimerem zbrojonym włóknami. Badana jest ewolucja uszkodzenia w takiej lekkiej konstrukcji. Połączenia stopu glinu AA5754 i termoplastycznego kompozytu zbrojonego włóknami węglowymi CF-PA66 są wykonywane przy użyciu epoksydowej warstwy adhezyjnej 1K-EP. Strefa kontaktu jest traktowana jako materiał interfejsowy. Celem badań jest analiza wpływu geometrii interfejsu na własności mechaniczne próbki. Metoda elementów skonczonych służy do symulacji skomplikowanych procesów zachodzących w połączeniu. Glin jest modelowany jako materiał sprężysto-plastyczny z liniowym wzmocnieniem izotropowym. Kompozyt polimerowy wykazuje ortotropowe zachowanie sprężyste. Przy dyskretyzacji warstwy adhezyjnej wykazującej uszkodzenie stosowane jest podejście interfejsu ciał stałych. Pokazano, że ewolucja uszkodzenia zależy od geometrii tego interfejsu. Praca zawiera analizę numeryczną procesu destrukcji próbek z kwadratowym, prostokątnym i okrągłym kształtem strefy adhezyjnej.

Słowa kluczowe*: uszkodzenie, analiza MES, lepkosprężystość, model uszkodzenia typu Lemaitre'a, połaczenie metal-kompozyt*

1. INTRODUCTION

Lightweight hybrid joints, like metal/polymer composite structures, have a great potential for application in a large number of engineering sectors. These material systems are opening up new possibilities for innovative product designs in automotive industry. The high specific stiffness and physico-chemical resistance of polymer composites are combined with traditional strength of metals in these advantageous combinations. The joints can be produced by ultrasonic metal welding or by means of adhesive bonding [1, 2]. Adhesive bonding is the most suitable method of joining both for metallic and non-metallic structures where strength and stiffness should be maximized at a minimum weight [3, 4]. As it is shown in experimental investigations the mechanical characteristics of adhesive joints mostly depend on the successful surface and substrate pretreatments [5, 6]. For the theoretical study the accurate calculation of the stress distribution in bonded joints and modeling of damage are key issues. There are analytical approaches for describing of stress distribution in a closed-form [7]. Some numerical strategy based on a finite element method are developed in order to model the stress distribution and damage evolution in adhesive joints in 3-dimensional case [8]. Composite/metal overlap joint is modeled as two thin three-dimensional solids. Adhesive/substrate and interface can be simulated as two sets of nodes [9].

In this contribution, the solid interface model [10] is applied to numerical simulate the adhesive zone. The adhesive interface is considered as a two dimensional layer in the three dimensional problem. The applications of the finite element method and solid interface approach to analyze the mechanical behaviour of the light weight engineering structures, like ultrasonic metall welded aluminum/fiber-reinforced

* Institute of Applied Mechanics, University of Kaiserslautern P.O. Box 3049, D-67653 Kaiserslautern, Germany;
e-mail: konchako@rhrk.uni-kl.de, ram@rhrk.uni-kl.de, barth@rhrk.uni-kl.de

polymer specimens is known [11, 12]. The von Mises elastoplastic model is used to simulate the welding interface.

In this paper, the simulation of a single overlapping shear-tensile specimen with adhesive bonding is considered. The joints of aluminium alloy 5754 (AA5754) and carbon fibre reinforced thermoplastic composite CF-PA66 is realized by means of an adhesion with an epoxy. Viscoelastic model with Lemaitre-type damage is applied in this article to simulate the contact zone. So, there are three model parts in the specimen of the joint: the polymer composite (matrix and fibre reinforcement), the metallic partner and an interface material in the joint adhesive zone.

2. COMPUTATION OF BULK MATERIALS

The material AA5754 is simulated as a elastoplastic material with isotropic hardening. The polymer composite CF-PA66 generally shows an orthotropic elastic behaviour.

2.1. Elastoplastic model with isotropic hardening

An elastoplastic bulk material law with isotropic hardening is used to model the aluminium plate [11, 12]. The total strain ε is split into

$$\varepsilon = \varepsilon^e + \varepsilon^p \tag{1}$$

separate the elastic part ε^e and the plastic part ε^p. Stresses are given as

$$\boldsymbol{\sigma} = \boldsymbol{\sigma}(\varepsilon^e, \alpha^p) \tag{2}$$

depending on the elastic strains and a plastic parameter α^p, accounting for irreversible plastic effects. In order to separate an elastic and a plastic range for loads above the yield limit, the von Mises yield function is proposed as

$$\Phi = \sqrt{\frac{3}{2}}\left|\boldsymbol{\sigma}^{\mathrm{dev}}\right| - \left[Y_0 + H^p \alpha^p\right] \tag{3}$$

where Y_0 is initial the yield stress, $|\boldsymbol{\sigma}^{\mathrm{dev}}|$ is the norm of the deviatoric part of the stress tensor and H^p is the linear hardening modulus.

The plastic evolution equations have the following form:

$$\dot{\varepsilon}^p = \dot{\gamma}\frac{\boldsymbol{\sigma}^{\mathrm{dev}}}{\left|\boldsymbol{\sigma}^{\mathrm{dev}}\right|}, \quad \dot{\alpha}^p = \dot{\gamma}\sqrt{\frac{2}{3}} \tag{4}$$

Here $\dot{\gamma}$ is a Lagrange multiplier, determined by the consistency condition during plastic flow.

2.2. Orthotropic elastic model

The orthotropic linear elastic model with two orthogonal directions of anisotropy $\boldsymbol{e}_1$ and $\boldsymbol{e}_2$ is applied for the computation of a second bulk material. So, two corresponding structure tensors $\boldsymbol{A}_1 = \boldsymbol{e}_1 \otimes \boldsymbol{e}_1$ and $\boldsymbol{A}_2 = \boldsymbol{e}_2 \otimes \boldsymbol{e}_2$ are introduced. In this case the free energy can be represented with regard to 7 invariants [13]:

$$\Psi = \Psi(i_\varepsilon, i_{\varepsilon A_1}, i_{\varepsilon A_2}) = (I_1, I_2, I_3, I_4, I_5, I_6, I_7)\,,$$

with

$$i_\varepsilon = \{I_1, I_2, I_3\}, \quad i_{\varepsilon A_1} = \{I_4, I_5\} = \{\varepsilon : \boldsymbol{A}_1, \varepsilon^2 : \boldsymbol{A}_1\},$$

$$i_{\varepsilon A_2} = \{I_6, I_7\} = \{\varepsilon : \boldsymbol{A}_2, \varepsilon^2 : \boldsymbol{A}_3\}.$$

The stresses are computed by differentiating the free energy:

$$\boldsymbol{\sigma} = \frac{\partial \Psi}{\partial \varepsilon} = \Phi_1 \mathbf{I} + \Phi_2 \boldsymbol{\varepsilon} + \Phi_3 \boldsymbol{\varepsilon}^2 + \Phi_4 \mathbf{A}_1 +$$

$$+\Phi_5 2[\boldsymbol{\varepsilon} \cdot \mathbf{A}_1]^{sym} + \Phi_6 \mathbf{A}_2 + \Phi_7 2[\boldsymbol{\varepsilon} \cdot \mathbf{A}_2]^{sym},$$

with

$$\Phi_1 = \frac{\partial \Psi}{\partial I_1} = \lambda I_1 + \alpha_1 I_4 + \alpha_2 I_6,$$

$$\Phi_2 = \frac{\partial \Psi}{\partial I_2} = 2\mu,$$

$$\Phi_3 = \frac{\partial \Psi}{\partial I_3} = 0,$$

$$\Phi_4 = \frac{\partial \Psi}{\partial I_4} = \alpha_1 I_1 + \beta_1 I_4 + \beta_3 I_6,$$

$$\Phi_5 = \frac{\partial \Psi}{\partial I_5} = 2\mu_1,$$

$$\Phi_6 = \frac{\partial \Psi}{\partial I_6} = \alpha_2 I_1 + \beta_3 I_4 + \beta_2 I_6,$$

$$\Phi_7 = \frac{\partial \Psi}{\partial I_7} = 2\mu_2;$$

λ, μ, α_i, μ_i and β_i are orthotropic material parameters; $\mathbf{I}$ is the identity tensor.

3. INTERFACIAL MATERIAL MODEL

As it is shown in the experimental works, an adhesive is defined as a polymeric substance with viscoelastic behaviour [3]. Therefore viscoelastic model with the Lemaitre-type damage is taken into account to model the properties of the interface adhesive material. The displacement jump $[\mathbf{u}]$ is split into an elastic part $[\mathbf{u}]^e$ and a viscous part $[\mathbf{u}]^{ve}$

$$[\mathbf{u}] = [\mathbf{u}]^e + [\mathbf{u}]^{ve} \tag{5}$$

where $[\mathbf{u}] = \mathbf{u}_{\Gamma+} - \mathbf{u}_{\Gamma-}$ is the jump across the adhesive interface Γ. The tractions of the interface are derived from the free energy function of the interface $\Psi^{if} = \Psi^{if}([\mathbf{u}], [\mathbf{u}]^e, d_i)$:

$$\boldsymbol{\tau} = \frac{\partial \Psi^{if}}{\partial [\mathbf{u}]} + \frac{\partial \Psi^{if}}{\partial [\mathbf{u}]^e} = \boldsymbol{\tau}^\infty + \boldsymbol{\tau}^m \tag{6}$$

The first part of the interface traction $\boldsymbol{\tau}^{\infty}$ is the traction of a parallel spring. The second part of the decomposition $\boldsymbol{\tau}^{m}$ is the traction of a serial arrangement of a damper and a spring (see [13] for details). The dependencies of the tractions are given as

$$\tau^{\infty} = \left[\sum_i [1-d_i]\mathbf{C}_i^{if,el,\infty}\right]\cdot[\mathbf{u}],$$
$$\tau^{m} = \left[\sum_i [1-d_i]\mathbf{C}_i^{if,el,m}\right]\cdot[\mathbf{u}]^{e}, \qquad i = s, t, n \tag{7}$$

where $\{s, t, n\}$ are the orthonormal interfacial directions, the elastic interfacial tangent stiffness tensor with respect to the parallel spring is $\mathbf{C}_i^{if,el,\infty}$ and to the damper system spring is $\mathbf{C}_i^{if,el,m}$. The damage parameter d_i is introduced, with $d_i \in [0, 1[$ and $\dot{d}_i > 0$, thus healing effects are excluded. It is incorporated in a Lemaitre-type damage context, see [14]. For $d_i \to 1$, the material tends to be fully damaged and is unable to bear any load. Exponential relations are chosen for the damage parameter:

$$d_i = 1 - \exp(j_i[\mu_{i(0)} - \mu_i]) \tag{8}$$

Here the parameter j_i is an intensity of damage evolution in i-direction, the value $\mu_{i(0)}$ is a damage threshold. The variable μ_i accounts for the progress of damage in i-direction. It is computed according to

$$\mu_i = \max\left(\bar{\mu}_i([\mathbf{u}], [\mathbf{u}]^{e}), \mu_{i(0)}\right),$$

and the so-called damage driving force is given by

$$\bar{\mu}_i = \frac{\partial \Psi^{if}}{\partial d_i}.$$

The constitutive assumption of viscoelasticity is given by the rate dependency

$$[\dot{u}_i]^{ve} = \frac{\tau_i^m}{\eta_i} = \frac{1-d_i}{T_i}\left[[u_i]-[u_i]^{ve}\right], \quad T_i = \frac{\eta_i}{c_i^m} \tag{9}$$

where η_i denotes to the viscosity in i-direction and T_i is the relaxation time.

4. NUMERICAL SIMULATION

The finite element method is used to simulate adhesive joints. The bulk materials are computed by means of standard continuum elements. In this paper the adhesive zone is modelled with a solid interface approach by using special interface elements. Solid interfaces are one geometrical dimension lower than the surrounding continuum, see [10]. Thus, to model interfaces in three dimensions, two dimensional interface elements are needed. For the determination of the displacements $\mathbf{u}$ and the displacement jumps $[\mathbf{u}]$ across the interface the principle of virtual work with virtual displacements $\hat{\mathbf{u}}$ and $[\hat{\mathbf{u}}]$ is used. The finite element approximation of the displacement jump and the test function jump [13] are given by

$$[\mathbf{u}]^{h}(\xi_1, \xi_2) = \mathbf{B}_{el}\cdot\mathbf{u}^{N}, \quad [\hat{\mathbf{u}}]^{h}(\xi_1, \xi_2) = \mathbf{B}_{el}\cdot\hat{\mathbf{u}}^{N},$$

where $\mathbf{u}^{N} = [\mathbf{u}_1, \mathbf{u}_2, \mathbf{u}_3, \mathbf{u}_4, \mathbf{u}_5, \mathbf{u}_6, \mathbf{u}_7, \mathbf{u}_8]^{T}$ and $\hat{\mathbf{u}}^{N} = [\hat{\mathbf{u}}_1, \hat{\mathbf{u}}_2, \hat{\mathbf{u}}_3, \hat{\mathbf{u}}_4, \hat{\mathbf{u}}_5, \hat{\mathbf{u}}_6, \hat{\mathbf{u}}_7, \hat{\mathbf{u}}_8]^{T}$ are the nodal displacements of the adjacent elements. The matrix B_{el} is the element operator matrix. The ansatz functions for the interface elements are introduced by

$$N_N(\xi_1, \xi_2) = \frac{1}{4}[1 + \xi_{1N}\xi_1][1 + \xi_{2N}\xi_2],$$

where the index N denotes the number of the node and ξ_{1N}, ξ_{2N} are the nodal coordinates in the element coordinate system. The interpolation variables are given by $\xi_1, \xi_2 \in [-1, 1]$.

Table 1

Mechanical properties of aluminum alloy sheet

AA5754			
Young's Modulus [GPa]	Yield Strength [MPa]	Ultimate Tensile Strength [MPa]	Ultimate Strain [%]
70.58	177	250	13.5

5. RESULTS AND DISCUSSION

The influence of interface geometry on the mechanical characteristics of adhesive overlapping tensile specimen is analyzed. Three different geometries of adhesive interfaces are considered: square, circle and rectangular geometry, which correspond to the coupling faces. All three interface geometries have the same area of 100 mm^2 and are placed in the centre of the overlapping zone, see Figure 1.

The free and remote part of a polymer composite CF-PA66 is clamped. The free part of a AA5754 metal sheet is subjected to an extension. The given displacement increment is u_x = 0.02 mm at each loadstep. We model the joint of aluminum sheet in a thickness of 1mm and also consolidated sheet of carbon fiber-reinforced polyamide 66 with a thickness of 2 mm. Size of the adhesive square is 10 mm × 10 mm, size of the rectangles 25 mm × 4 mm, the circle has a radius of 5.64 mm. In case of the square interface, 3108 bulk and 100 interface elements are used. In case of a rectangle, the model contains 3644 elements, including 160 interface elements. The third simulation for the circle interface uses 3834 elements, 140 of which are in the interface layer.

Table 2

Orthotropic parameters of carbon fiber reinforced polymer

CF-PA66 [MPa]								
λ	α_1	α_2	β_1	β_2	β_3	μ	μ_1	μ_2
4555	–3263	–3263	51466	51466	7524	–1000	1900	1900

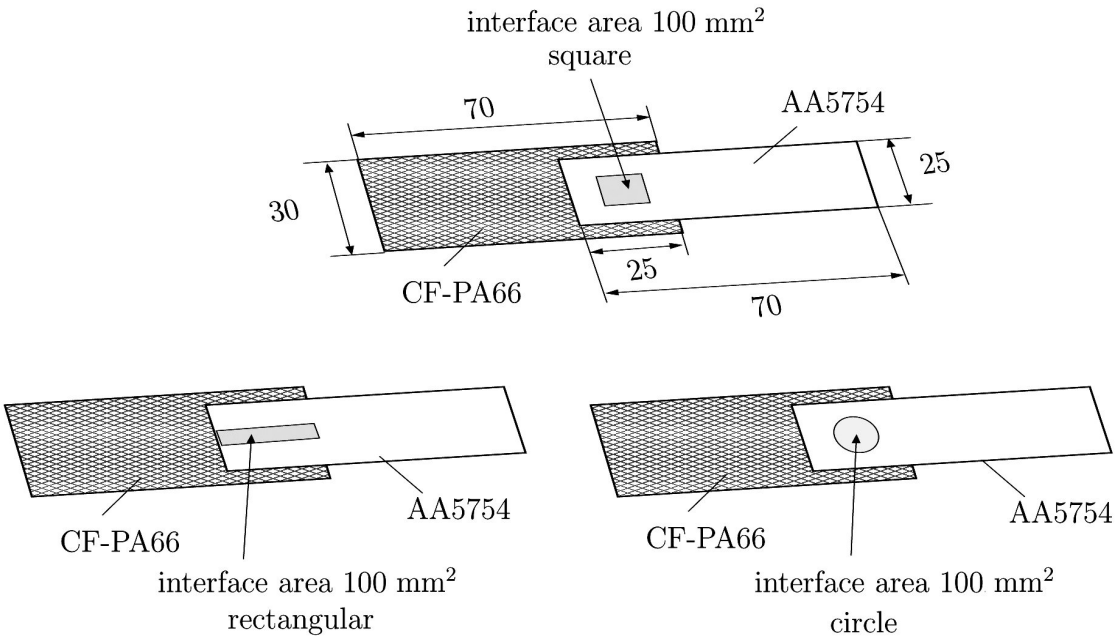

Fig. 1. Geometry of adhesive AA5754/CF-PA66 joints

The numerical analysis of the lightweight strictures is based on the investigation of force-displacement relations. First of all, we would like to demonstrate the large impact of interface material model onto the mechanical behaviour of the entire specimen. Figure 2 shows the influence of different material models the global force-displacement curves. The figure contains three simulated force-displacement curves of metal/fibre-reinforced polymer tensile joints for the cases of ideal interface, elastoplastic interface and viscoelastic interface model. As can be seen from the figure, the force-displacement curve of the corresponding AA5754/CF-PA66 joint specimen with an ideal interface (with no displacement jump, modelling of the perfect contact between metal and polymer composite) contains the zone of elasticity and the zone of plastic strain of the material. At the same time, the application of the elastoplastic model with the Lemaitre-type damage or the viscoelastic model with the Lemaitre-type damage to the simulation of AA5754/CF-PA66 joint enables us to speak about existence of the damage region as well (the zone of damage). The source of the interface parameters in the case of application of elastoplastic model was the experimentally measured force-displacement curve of ultrasonic welded AA5754/CF-PA66 joint, see [12, 15]. The adhesive interfacial material parameters (viscoelastic interface) are: Young's Modulus E = 1700 MPa, viscosity $\eta_s = \eta_t$ = 319.55 MPa·s, η_n = 850 MPa·s, damage threshold in i-direction $\mu_i(0) = 38 \cdot 10^{-2}$ MPa·m, intensity of damage evolution $j_i = 23.5 \cdot 10^{-2}$ [MPa·m]$^{-1}$, $i = s, n, t$. The material constants of AA5754 and CF-PA66 have been described in [11, 12] and are reported in Table 1 and 2.

A comparison of the different computational interface models indicates that the interface material has a considerable impact upon the specimen, reducing its elastic properties and initiating the zone of damage. In the zone of elastic deformations, the interface layer leads to a reduction of elasticity of the entire specimen as compared to the specimen with an ideal interface. Therefore, Young's modulus and Poisson's ratio of the interface were numerically selected such that the slope of the graph of the force-displacement in the elastic zone was smaller than that of the specimen with an ideal interface. Initial yield stress and hardening modulus of the interface were selected such that the zone of irreversible deformations is developed in the same manner as for an ideal interface. Damage constants of the interface were selected as to realize a mechanical behaviour with Lemaitre-type damage. So, despite the fact that the size of the interface layer corresponds to an intermediate layer, the influence of its parameters onto the mechanical behaviour of the entire specimen is significant.

The application of a viscoelastic model with Lemaitre type of damage to adhesive joints is considered in detail.

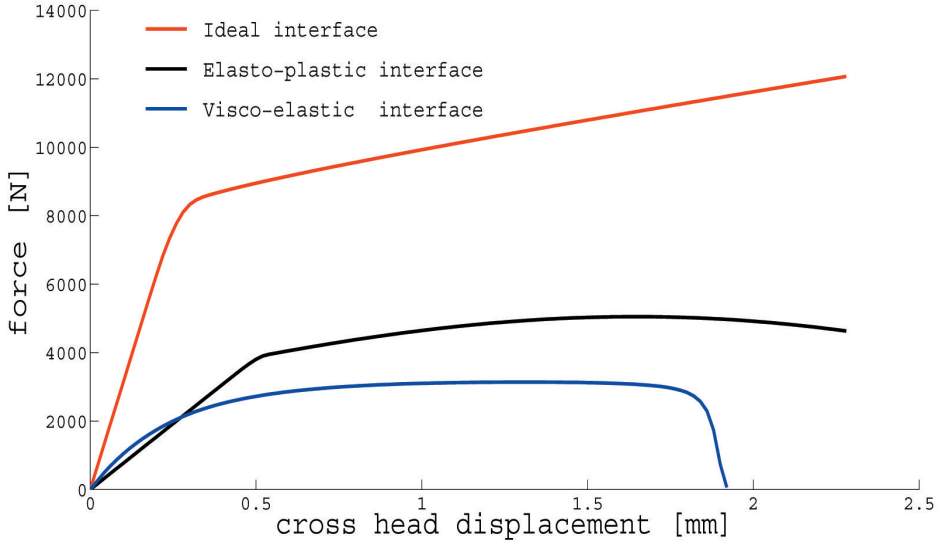

Fig. 2. Simulated force-displacement curves for different interfacial models

Figure 3 reflects the influence of loading rates on the characteristics of the specimen. The joint has the same given extension of $\Delta u = 0.02$ mm in each time increment Δt for all simulations. The graph demonstrates the influence of viscosity on the mechanical parameters of the specimen.

The influence of joint's geometry on the mechanical characteristics of specimen can be see in Figure 4. It contains three simulated force-displacement curves of aluminum/fiber-reinforced polymer tensile joints. The loading rate corresponds the case of $\Delta u = 0.02$ mm, and $\Delta t = 0.2$ s. It can be observed in the graphs a region of viscoelastic behaviour, a zone of plastic flow and a damage response for all three geometries. Secondly, the level of maximal loading is the same for all three joints, but the damage influence is first found in specimens with square interface. The fracture domain develops more actively in this specimen in comparison with the other two geometries.

The state of the interface can be analyzed with help of the interface traction distribution. The direction of the local interface coordinate system $\{s, t, n\}$ is changing with nodal position of the interface elements. Therefore the distribution of the interface mechanical parameters in the whole welding area is analyzed. The resolved shear stress in the adhesive surface can be computed by means of the following form:

$$\tau_{st} = \sqrt{\tau_s^2 + \tau_t^2}.$$

The numerical analysis of the maximal value of τ_{st} in the adhesive areas shows an increase of the traction in all interfaces for 0 mm $< u <$ 1.4 mm for square and rectangle joints, and 0 mm $< u <$ 1.54 mm for circle geometry.

The traction is the highest in a circle interface and minimal in a square interface at each loadstep. However, the interval of the traction growth is wider for circle geometry: the traction achieves its highest value of ~32 MPa for $u \simeq 1.26$ mm. The circle interface holds this traction approximately the next 30 loadsteps until $u \simeq 1.86$ mm. After that the shear stress τ_{st} decreases quickly.

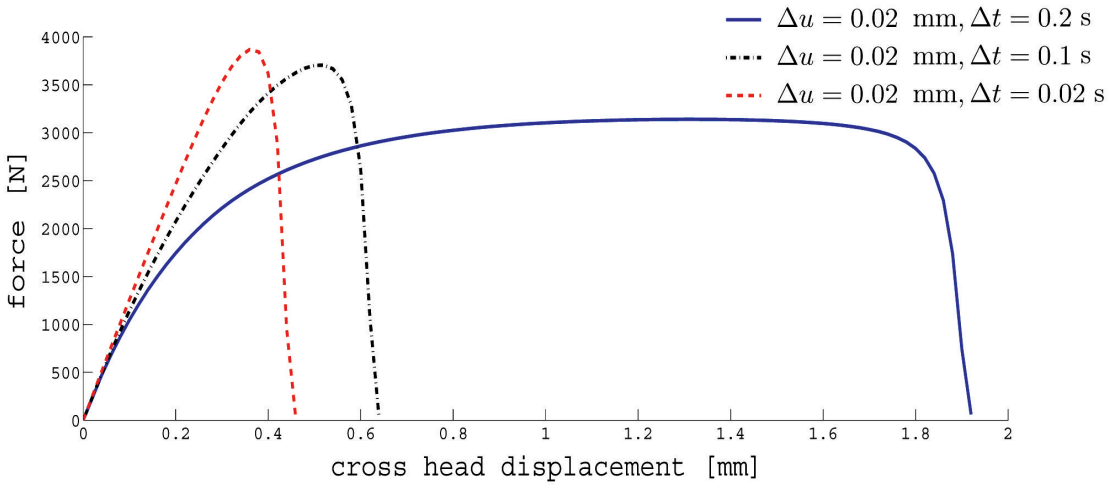

Fig. 3. Simulated force-displacement curves for different loading rates (square interface geometry)

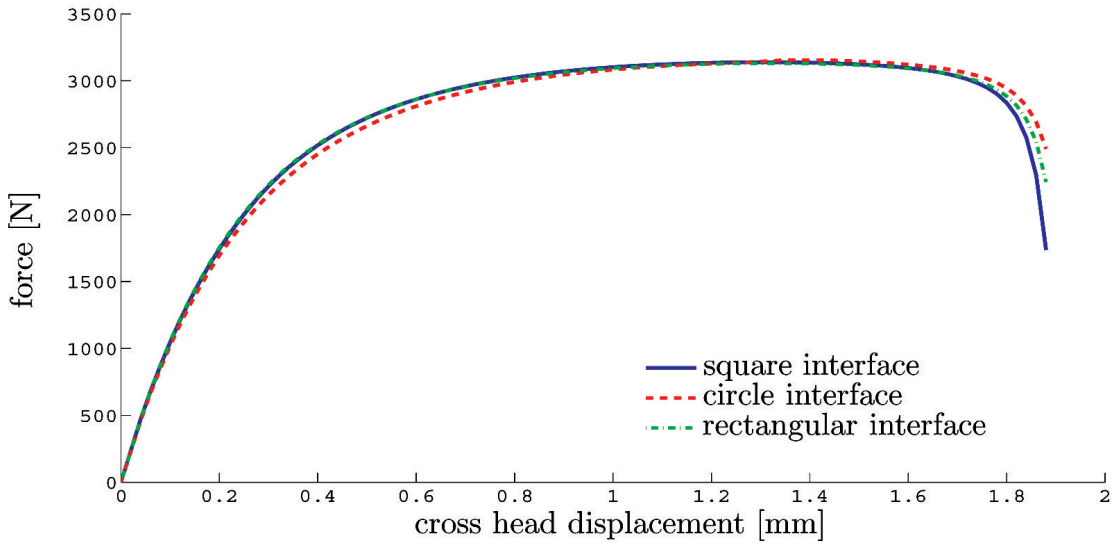

Fig. 4. Force-displacement curves of adhesive AA5754/CF-PA66 joints

At the same time the joint with square interface has an area of high traction ~27 MPa while 1.24 mm < u < 1.5 mm. Then we observe the falling of the resolved shear stress τ_{st}. Figure 5 shows the distribution of the shear stress τ_{st} in the adhesive zone for u = 1.5 mm. The zone of maximal traction is placed in the centre of interface. This is the state when fracture begins. More than 80% of interface area experiences the maximal value of τ_{st}. At the next loadstep the shear stress τ_{st} decreases.

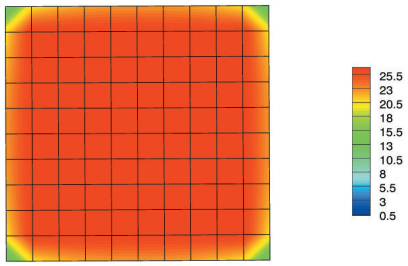

Fig. 5. Distribution of traction τ_{st} in square joint area, u = 1.5 mm

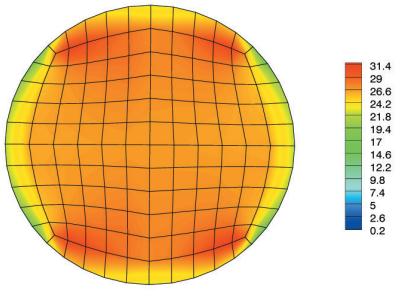

Fig. 6. Distribution of traction τ_{st} in circle joint area, u = 1.5 mm

Figure 6 depicts the distribution of the shear stress τ_{st} in the circle surface for the same step of the loading – u = 0.5 mm. As it is obvious from the graph, that the peak value occurs in the boundary part of the interface shifted in the direction of loading. The specimen is in a state of plastic deformation. Further loading causes the development and expansion of the region of maximal stress into the center of the interface.

The failure evolves into the joint area due to the action of a shear stress. At the initial stage of damage evolution, with 0.4 mm < u < 0.8 mm, a shear stress in the joints initiates a zone of high damage at the boundary area shifted in the direction of loading. An increase of the shear stress causes the growth of the damage zone into the center of the interface. Further loading contributes to the development and extension of the region of high damage into the interface. The maximal damage value

$$d_{st}^{\max} = \max\left(\sqrt{d_s^2 + d_t^2}\right)$$

in joint area is presented in Figure 7. The diagram shows the maximal damage d_{st} for square and circle interfaces when the cross head displacements is 0.6 mm, 1.4 mm, 1.8 mm and 2.0 mm. The maximal damage value develops rather similarly in initiate stage of the loading. The damage value is approximately 0.2 for both cases in the area of viscoelastic behaviour and about 0.32 in the area of irreversible strain. The formation of the failure domain is reflected by an increase of the damage parameter when $u \geq 1.6$ mm. The growth of the damage d_{st} in the corresponding area is more than 0.52 for the case of a circular geometry and more than 0.57 in a square interface. The increase of the damage values in the fracture zone ($u \geq 1.9$ mm) is higher than 0.88 in the case of a square interface and 0.77 in circle joint. With further loading, the values of the damage d_{st} grow. The region of maximum damage is located in the center of the overlap.

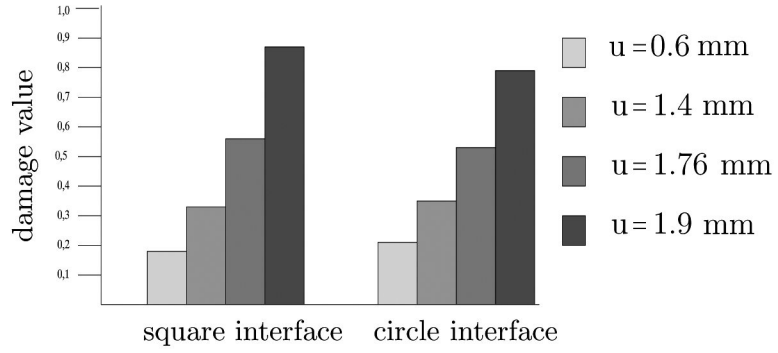

Fig. 7. Maximal damage value d_{st} in joint area

The distribution of d_{st} in the rectangular interface is between the damage value of the square and the circle geometry. In all three cases, the value of d_{st} increases monotonously with u. The formation of a failure domain occurs when both of damage parameters (d_s or d_t) tend to 1. So, fracture develops more actively in the specimen with square interface geometry in comparison to the other two geometries. The damage in the adhesive domain evolves a bit slower in the case of rectangle geometry, and rather slowly in the circle joint. The difference between the damage values in the case of square and circle geometry is ~11% at the 100^{th} loadstep (when u = 2.0 mm). Therefore, the numerical analysis of the damage evolution in the adhesive zone shows that damage evolves slower in the case of circular geometry.

6. CONCLUSION

The investigation of the mechanical properties of adhesive lightweight joints made from an aluminum alloy and a fiber-reinforced polymer is based on the application of the viscoelastic model with Lemaitre-type damage and the solid interface approach. The aluminum alloy is simulated using the von Mises elastoplastic model with isotropic hardening. The modeling of polymer material is realized by means of orthotropic linear elastic model taking into account two direction of anisotropy. The phenomenological modeling of the interface characteristics allows us to compute the global force-displacement curves for adhesive joints with different interface properties and geometries. It is analyzed the behaviour of specimens with ideal interface, elastoplastic interface and viscoelastic interface. First of all we can conclude that the interface material has a considerable impact upon the whole specimen, reducing its elastic properties and initiating the zone of damage. The numerical results of the application of viscoelastic model with Lemaitre-type damage to adhesive domain show the direct dependency of the mechanical behavior on the loading rate. The influence of adhesive geometry is analyzed for the cases of square, circle and rectangular shapes of the adhesive joint. Three characteristics of the mechanical behavior of the specimen are observed: the region of viscoelastic behavior, the plastic zone and the damage domain. We have observed a weak dependency of the mechanical behavior on the adhesive geometry. Numerical analysis of the distribution of interfacial traction and damage values shows that the specimen with a square interfacial area exhibits the most intensive damage evolution. The joint with circular area can support the highest loading as compared to other geometries under consideration.

Acknowledgments

The authors thank the German Research Foundation (DFG) for the financial support within the Research Unit (FOR) 524 "Manufacturing, Characterization and Simulation of Welded Lightweight Structures of Metal/Fibre-reinforced Polymer Composites" at the University of Kaiserslautern.

References

[1] Balle F., Wagner G., Eifler D. 2009, *Ultrasonic Metal Welding of Aluminium Sheets to Carbon Fibre Reinforced Thermoplastic Composites*. Advanced Engineering Materials, 11, pp. 35–39.

[2] Velthuis R., Koetter M.P., Geiss P.L., Mitschang P., Schlarb A.K. 2007, *Lightweight Structures Made of Metal and Fiber-Reinforced Polymers*, Kunststoffe international, 11, pp. 22–24.

[3] Baldan A. 2004, *Adhesively-bonded Joints and Repairs in Metallic Aloys*. Polymers and Composite Materials: Adhesives, Adhesion Theories and Surface Pretreatment J. of Mater. Sci., 39, pp. 1–49.

[4] da Silva, Lucas F.M., Adams R.D. 2007, *Adhesive joints at high and low temperatures using similar and dissimilar adherends and dual adhesives*. International Journal of Adhesion and Adhesives, 27, pp. 216–226.

[5] Brodyanski M., Geiss P.L., Kopnarski M., Passlack S., Possart G., Presser M., Steinmann P. 2009, *Micro-macro Characterisation of DGEBA-based Epoxies as a Preliminary to Polymer Interphase Modelling*. International Journal of Adhesion and Adhesives, 29, pp. 478–487.

[6] Sihn S., Miyano Y., Nakada M., Tsai SW. 2003, *Time- and Ttemperature-dependent Failures of a Metal-to-Composites Bonded Joint with PMMA Adhesive Material*. J. of Composite Materials 37, pp. 35–54.

[7] Deheeger A., Mathias J.D., Grediac M. 2009, *A closed-form solution for the thermal stress distribution in rectangular metal/composite bonded joints*. International Journal of Adhesion and Adhesives, 29, pp. 515–524.

[8] Ribeiro F.L., Borges L., d'Almeida J.R.M. 2011, *Numerical stress analysis of carbon-fibre-reinforced epoxy composite single-lap joints*. International Journal of Adhesion and Adhesives, 31 pp. 331–337.
[9] Derewonko A. 2009, *Prediction of the failure metal/composite bonded joints*. Int. J. Comput. Mater. Sci, 45, pp. 735–738.
[10] Steinmann P., Betsch P. 2000, *A localisation capturing FE-interface based on regularized strong discontinuties at lage inelastic strain*. Int. J. Solids Struct, 37, pp. 4061–4082.
[11] Utzinger J., Bos M., Floeck M., Menzel A., Kuhl E., Renz R., Friedrich K., Schlarb A., Steinmann P. 2008, *Computational modelling of thermal impact welded peek/steel single lap tensile specimens*. Int. J. Comput. Mater. Sci., 41, pp. 287–296.
[12] Konchakova N., Balle F., Barth F.J., Mueller R., Eifler D., Steinmann P. 2010, *Finite Element Analysis of an Inelastic Interface in Ultrasonic Welded Metal/Fibre-Reinforced Polymer Joints*. Int. J. Comput. Mater. Sci, 50, pp. 184–190.
[13] Utzinger J. 2008, *Analysis and Computation of Solid Interfaces on the Meso Scale*. PhD thesis, TU Kaiserslautern, Germany.
[14] Lemaitre J., *A Course on Damage Mechanics*. Springer, 1994.
[15] Konchakova N., Mueller R., Barth F.J., Balle F., Eifler D. 2010, *Damage Evolution in Ultrasonic Welded Aluminum/Fibre-Reinforced Polymer Joints with Different Welding Geometries*. Supplemental Proc. TMS Annual Meeting 2011, vol. 2: Materials Fabrication, Properties, Characterization and Modelling, pp. 601–608.